Electronic Supplementary Information

Amorphous Palladium-Based Nanoparticles as Highly Active Electrocatalysts for Ethanol Oxidation

Yufeng Zhang[a], Jinjie Fang[a], Lipeng Zhang[a], Dong Wei[a], Wei Zhu[a*], Zhongbin Zhuang[a,b*]

[a.] *State Key Lab of Organic-Inorganic Composites and Beijing Advanced Innovation Center for Soft Matter Science and Engineering, Beijing University of Chemical Technology, Beijing 100029, China.*
[b.] *Beijing Key Laboratory of Energy Environmental Catalysis, Beijing University of Chemical Technology, Beijing 100029, China.*

Chemicals.

Ethanol (99.9%, Aladdin), oleylamine (OAm, 80-90%, Aladdin), borane tert-butylamine complex (BTB, 97%, Adamas Reagent Co. Ltd), palladium acetylacetonate ($Pd(acac)_2$, 99%, Aladdin), potassium hydroxide (KOH, 99%, Aladdin), tri-n-octylphosphine (TOP, 90%，Aladdin). All regents are used as received without further purification.

Synthesis of *a*-$PdP_{0.1}$ nanoparticles.

8 mL of OAm and 0.04 mmol of $Pd(acac)_2$ were mixed together in a three flask and heated to 60 °C under N_2. After stirring evenly, 0.8 mL of TOP was injected and stirred for 10 min. Then, it was heated to 300 °C and kept at this temperature for 80 min. The product was collected by ethanol wash and centrifugation, and finally dispersed in cyclohexane.

Synthesis of *c*-Pd nanoparticles.

8 mL of OAm and 0.04 mmol of $Pd(acac)_2$ were mixed together in a three flask and heated to 120 °C under N_2. After stirring evenly, 40 mg of BTB dissolved in 1 mL of OAm was injected. After 60 min of reaction, the product was collected by ethanol wash and centrifugation, and finally dispersed in cyclohexane.

Loading the nanoparticles on carbon.

16.6 mg of carbon (Vulcan XC-72, Carbot Co) was dissolved in 20 mL of cyclohexane and stirred evenly under ultrasonic condition. Then, 2 mL of the synthesized nanoparticle cyclohexane dispersion, containing approximately 4.2 mg of nanoparticles, was added to the suspension. After 1 h of ultrasound and 24 h of stirring, it was dried at 60 °C.

Physical Characterizations.

The X-ray powder diffraction (XRD) patterns were obtained on a Rigaku D/Max 2500 VB2+/PC X-ray powder diffractometer equipped with Cu Kα radiation (λ = 0.154 nm) operating at 40 kV and 40 mA at a scanning rate of 10° min^{-1}. The transmission electron microscopy (TEM) images were acquired on a JEOL JEM-1230 transmission electron microscope. High-resolution TEM (HRTEM) and energy-dispersive X-ray spectroscopy (EDS) were performed on a Talos F200X transmission electron

microscope. The XPS spectra were recorded on a Thermo Fisher ESCALAB 250Xi XPS system with a monochromatic Al Kα X-ray source. The binding energies derived from XPS measurements were calibrated to the C 1s at 284.8 eV. The elemental analyses were done by a Thermo-Fisher ICAP 6300 Radial inductively coupled plasma optical emission spectroscopy (ICP-OES) instrument.

Electrochemical tests.

The electrochemical tests were carried out in a three-electrode cell controlled by an electrochemical workstation (CHI 760E). A saturated calomel electrode (SCE) was used as the reference electrode, and a graphite electrode was used as the counter electrode. The catalysts ink were drop-casting on a glassy carbon electrode and used as the working electrode. The catalyst ink was prepared by dispersing 2 mg of catalyst in the mixed solution of isopropanol (750 μL), water (240 μL), and Nafion solution (20 μL, Alfa Acesar, 5 wt%). 9 μL of the ink was dropped onto a glassy carbon electrode (5 mm in diameter, PINE instruments). The Pd loadings were controlled as 11 $\mu g \cdot cm^{-2}$. The electrolytes for the EOR reaction were 1.0 M ethanol and 1.0 M KOH.

Electrochemical active surface areas (ECSAs) of the Pd based catalysts were calculated by the equation of

$$ECSA = Q / (m \cdot C)$$

where Q is the amount of charge needed to reduce surface oxidized Pd, m is the Pd mass of catalysts on the electrode, and C is the constant of 420 $\mu C \cdot cm_{Pd}^{-2}$.

ECSA of Pt/C was calculated by the charger transferred in the H_{upd} region using a constant of 210 $\mu C\ cm_{Pt}^{-2}$.

Electrochemical *in-situ* FT-IR experiments.

A Nicolet iS50 FT-IR transform infrared spectrometer equipped with a mercury cadmium telluride detector cooled with liquid nitrogen was employed in the *in-situ* electrochemical study. A calcium fluoride window and an *in-situ* EC-IR thin cell were applied in the test. The working electrode was a glassy carbon electrode (10 mm in diameter) with a catalyst loading of 50 $\mu g \cdot cm^{-2}$. The SCE and Pt wire were used as reference electrode and counter electrode, respectively. The working electrode was pressed onto the calcium fluoride window with a gap less than 10 μm when collecting

IR spectrum. The electrolyte was 0.1 M KOH with 1.0 M ethanol. The reference spectrum was collected at 0.1 V. The spectrum at each potential was normalized by the reference spectrum as follows:

$$\Delta R/R=(R(ES)-R(ER))/(R(ER))$$

R(ER) and R(ES) were the spectrum at reference potential and tested potential, respectively.

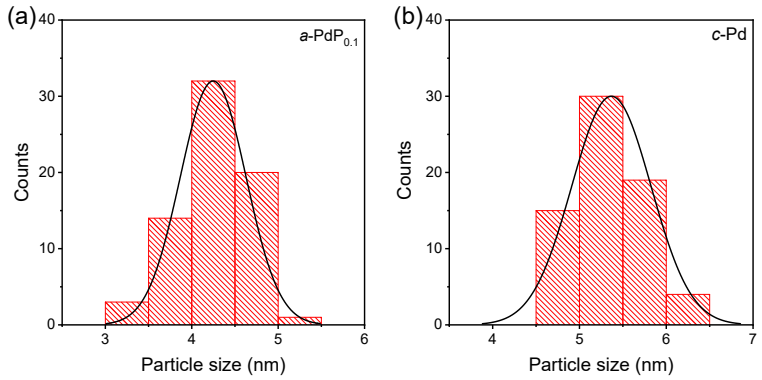

Figure S1. The size distribution histogram of (a) *a*-$PdP_{0.1}$ and (b) *c*-Pd.

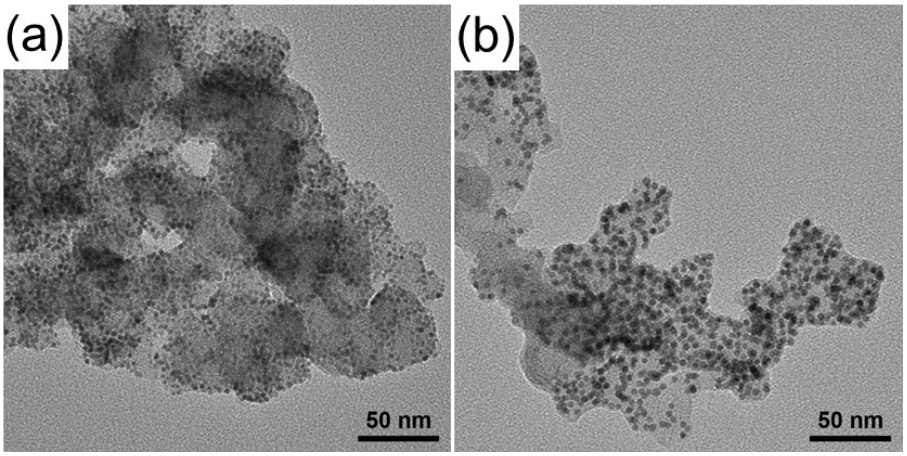

Figure S2. TEM image of (a) *a*-$PdP_{0.1}$/C and (b) *c*-Pd/C.

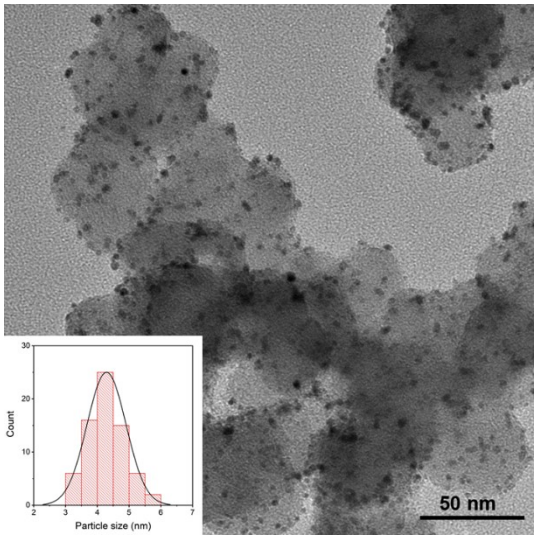

Figure S3. TEM image of the commercial Pt/C. Inset is the size distribution histogram of Pt.

The particle size of Pt was about 4.3 nm, which was similar to that of *a*-$PdP_{0.1}$ or *c*-Pd.

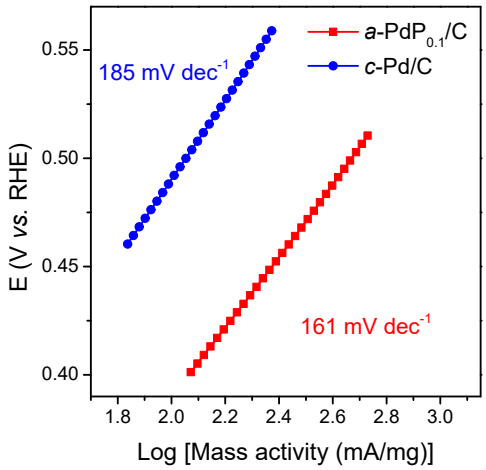

Figure S4. Tafel plots of *a*-$PdP_{0.1}$/C and *c*-Pd/C.

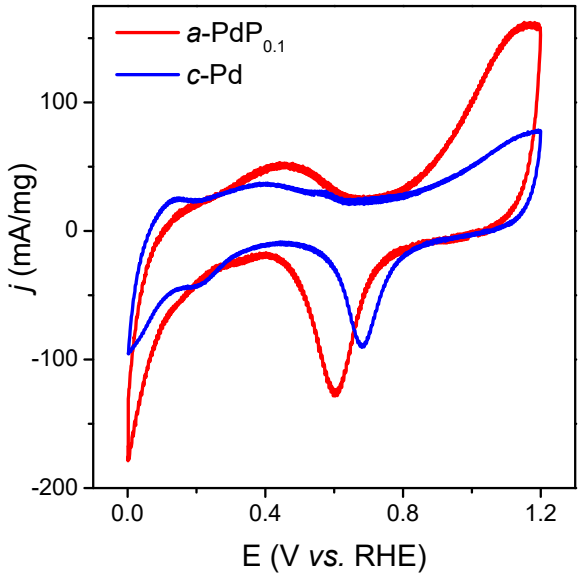

Figure S5. CV curves of *a*-$PdP_{0.1}$/C and *c*-Pd/C obtained in 1.0 M KOH at a scan rate of 50 mV s^{-1}.

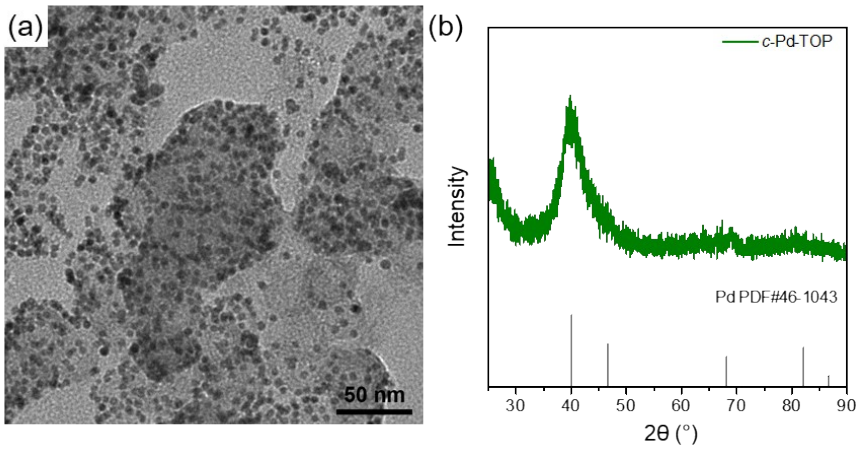

Figure S6. Characterization of *c*-Pd-TOP. (a) TEM image. (b) XRD pattern.

The *c*-Pd-TOP was obtained by ligand exchanging of the as-obtained c-Pd at 180 °C for 30 min.

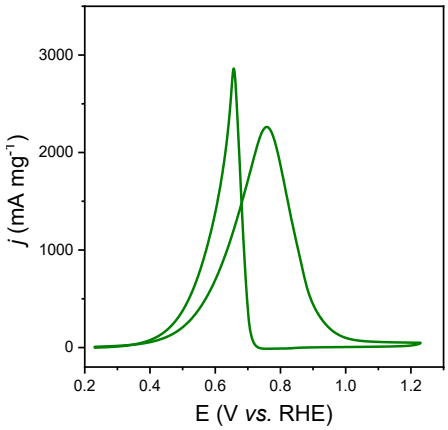

Figure S7. The EOR polarization curve of *c*-Pd-TOP obtained in 1.0 M KOH with 1.0 M ethanol at a scan rate of 50 mV s^{-1}.

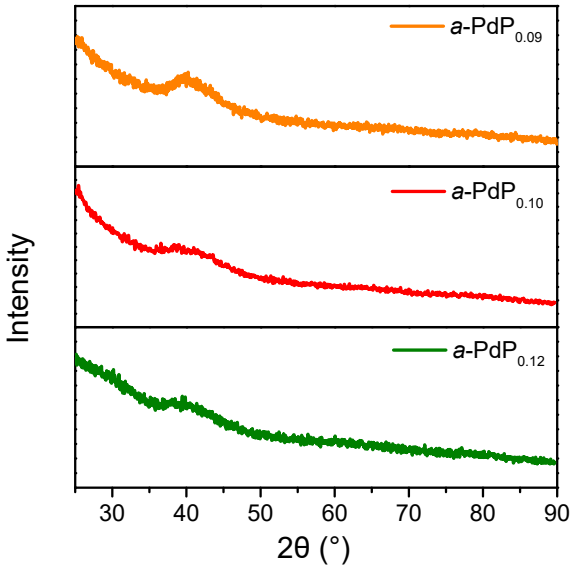

Figure S8. XRD patterns of the Pd-P alloy nanoparticles with different content of P.

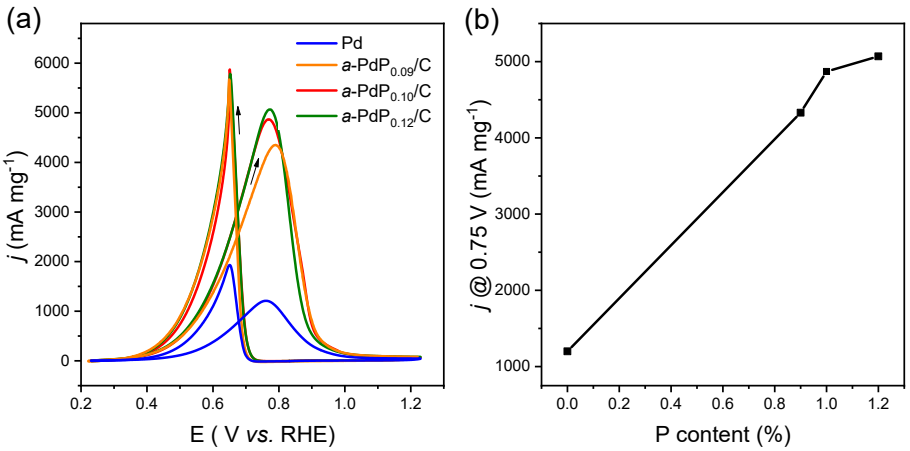

Figure S9. (a) The polarization curves of the Pd-P alloy nanoparticles with different content of P obtained in 1.0 M KOH with 1.0 M ethanol at a scan rate of 50 mV s^{-1}. (b) Mass activities at 0.75 V Pd-P alloy nanoparticles with different content of P.

Table S1. Summary of the EOR performance of Pd-based catalysts at 0.75 V.

Catalysts	Mass activity (mA mg^{-1})	
a-$PdP_{0.1}$	4851	This work
c-Pd	1191	This work
c-Pd-Ni-P@*a*-Pd-Ni-P nanoplate	2500	[1]
PdP nanosheet	2300	[2]
P doped PdNiCu	1050	[3]
Pd@CoP NSs/CFC	1000	[4]
Pd-Ni-P	3500	[5]
Pd/C-N,S,P	1200	[6]
2D PdAg Alloy Nanodendrites	1500	[7]
Pd Nanosheets	700	[8]
Pd/amorphous-$SrRuO_3$	1300	[9]

1. P. F. Yin, M. Zhou, J. Chen, C. Tan, G. Liu, Q. Ma, Q. Yun, X. Zhang, H. Cheng, Q. Lu, B. Chen, Y. Chen, Z. Zhang, J. Huang, D. Hu, J. Wang, Q. Liu, Z. Luo, Z. Liu, Y. Ge, X. J. Wu, X. W. Du and H. Zhang, *Adv. Mater.*, 2020, **32**, e2000482.
2. H. Lv, Y. Teng, Y. Wang, D. Xu and B. Liu, *Chem. Commun.*, 2020, **56**, 15667-15670.
3. D. Chen, R.-H. Zhang, Q.-Y. Hu, Y.-F. Guo, W. Zhan, S.-N. Chen, X.-W. Zhou and Z.-X. Dai, *ACS. Appl. Energy Mater.*, 2019, **2**, 5525-5533.
4. S.-H. Ye, J.-X. Feng and G.-R. Li, *ACS Catal.*, 2016, **6**, 7962-7969.
5. L. Chen, L. Lu, H. Zhu, Y. Chen, Y. Huang, Y. Li and L. Wang, *Nat. Commun.*, 2017, **8**, 14136.
6. K. Yu, Y. Lin, J. Fan, Q. Li, P. Shi, Q. Xu and Y. Min, *Catalysts*, 2019, **9**, 114.
7. W. Huang, X. Kang, C. Xu, J. Zhou, J. Deng, Y. Li and S. Cheng, *Adv. Mater.*, 2018, **30**, 1706962-1706968.
8. M. Yang, M. Pang, J. Chen, F. Gao, H. Li and P. Guo, *ACS Appl. Mater. Interfaces*, 2021, **13**, 9830-9837.
9. X. Wu, J. He, M. Zhang, Z. Liu, S. Zhang, Y. Zhao, T. Li, F. Zhang, Z. Peng, N. Cheng, J. Zhang, X. Wen, Y. Xie, H. Tian, L. Cao, L. Bi, Y. Du, H. Zhang, J. Cheng, X. An, Y. Lei, H. Shen, J. Gan, X. Zu, S. Li and L. Qiao, *Nano Energy*, 2020, **67**, 104247.